Journal of Physics: Conference Series **706** (2016) 042007 doi:10.1088/1742-6596/706/4/042007

Pasta phases in core-collapse supernova matter

Helena Pais, Silvia Chiacchiera, Constança Providência

CFisUC, Department of Physics, University of Coimbra, 3004-516 Coimbra, Portugal

E-mail: pais.lena@uc.pt, silvia@teor.fis.uc.pt, cp@fis.uc.pt

Abstract. The pasta phase in core-collapse supernova matter (finite temperatures and fixed proton fractions) is studied within relativistic mean field models. Three different calculations are used for comparison, the Thomas-Fermi (TF), the Coexisting Phases (CP) and the Compressible Liquid Drop (CLD) approximations. The effects of including light clusters in nuclear matter and the densities at which the transitions between pasta configurations and to uniform matter occur are also investigated. The free energy and pressure, in the space of particle number densities and temperatures expected to cover the pasta region, are calculated. Finally, a comparison with a finite temperature Skyrme-Hartree-Fock calculation is drawn.

1. Introduction

The complex structure of nuclear matter in the density region approaching $\rho_0 \sim 0.16$ fm^{-3} (central density of heavy nuclei) at finite temperature ($T < 20$ MeV) critically affects many astrophysical and nuclear physics phenomena. At low densities, the frustrated system called "pasta phase", caused by the competition between the Coulomb interaction and the strong force, appears, and is constituted by different geometrical configurations, as the density increases [1, 2, 3, 4, 5, 6, 7, 8, 9].

The main interest in the pasta phase in core-collapse supernovae (CCSN) is that the neutrino opacity, which plays an important role in the development of a shock wave during the supernova collapse, is affected by its presence [2, 10, 11]. At very low densities (up to 0.001 times the saturation density), light nuclei (deuterons, tritons, helions, α-particles) can appear [12, 13, 14, 15, 16, 17], and, like the pasta phase, can modify the neutrino transport, which will have consequences in the cooling of the proto-neutron star [18, 19].

Following our previous works (see e.g. [9] and references therein), we use the Thomas-Fermi (TF) approximation, where the surface effects are treated self-consistently, in the framework of relativistic mean field (RMF) models, to calculate the pasta phase for a fixed proton fraction, several temperatures and densities. Besides TF, we use the coexisting-phases (CP) method, which is numerically much faster than the TF one, and where the Gibbs equilibrium conditions are used to get the lowest free energy state, and the surface and Coulomb terms are added "by hand" (see e.g. [17]). Within this method, we also include the effect of light clusters. The compressible liquid drop (CLD) model is also considered. Unlike the CP approximation, this method takes into account both the Coulomb and surface terms in the minimization of the total energy of the system. For more details on the present work, the reader should refer to Ref. [20].

2. Formalism

We consider a system of baryons, with mass M interacting with and through an isoscalar-scalar field ϕ with mass m_s, an isoscalar-vector field V^μ with mass m_v and an isovector-vector field $\mathbf{b}^\mu$ with mass m_ρ. When describing *npe* matter we also include a system of electrons with mass m_e. Protons and electrons interact through the electromagnetic field A^μ. We use the FSU parametrization [21], expected to describe well the crust [9], even if it does not describe a 2 $M_\odot$ neutron star. This parametrization also includes a nonlinear $\omega\rho$ coupling term, which affects the density dependence of the symmetry energy. We consider the mean field approximation, where the thermodynamic quantities of interest are given in terms of the meson fields, which are replaced by their constant expectation values. We also consider matter with fixed proton fraction that is neutrino free, and hence the neutrino pressure and energy density are zero [22].

We use the same prescription as in [17] to include light clusters ($d \equiv{}^2$H, $t \equiv{}^3$H, $\alpha \equiv{}^4$He, $h \equiv{}^3$He) in the model. The α particles and the deuterons are described as in [12]. More realistic parametrizations for the couplings of the light clusters have been proposed in [12, 15], which should be implemented.

2.1. Thomas-Fermi, Coexisting Phases and Compressible Liquid Drop approximations

We use the Thomas-Fermi (TF) approximation to describe the nonuniform *npe* matter inside the Wigner-Seitz unit cell, that is taken to be a sphere, a cylinder or a slab in three, two, and one dimensions [22, 23, 9]. In this approximation, *npe* matter is assumed locally homogeneous and at each point its density is determined by the corresponding local Fermi momenta. In 3D we consider spherical symmetry, in 2D we assume axial symmetry around the z axis, and in 1D reflexion symmetry is imposed. In the TF approximation, fields are assumed to vary slowly so that baryons can be treated as moving in locally constant fields at each point [4]. In this approximation, the surface effects are treated self-consistently. Quantities such as the energy and entropy densities are averaged over the cells, when shown in figures, see e.g. Ref. [20]. The free energy and pressure are calculated from these two thermodynamical functions, using the usual expressions, see e.g. Ref. [24].

In the Coexisting Phases (CP) method, matter is organized into separated regions of higher and lower density, the higher ones being the pasta phases, and the lower ones a background nucleon gas. The interface between these regions is sharp. Finite size effects are taken into account by a surface and a Coulomb terms in the energy density [17].

In this approximation, the Gibbs equilibrium conditions are imposed to get the lowest energy state, and, for a temperature $T = T^I = T^{II}$, are written as

$$\begin{aligned} \mu_n^I &= \mu_n^{II}, \\ \mu_p^I &= \mu_p^{II}, \\ P^I &= P^{II}, \end{aligned} \tag{1}$$

where I and II label the high- and low-density phases, respectively. When clusters are present, there are equilibrium conditions for them too [17].

In the Compressible Liquid Drop model [25, 26, 18, 27], the equilibrium conditions of the system are derived from the minimization of the total free energy [25], including the surface and Coulomb terms. This minimization is done with respect to four variables: the size of the geometric configuration, r_d, the baryonic density in the high-density phase, ρ^I, the proton density in the high-density phase, ρ_p^I, and the volume fraction in the high-density phase, f. The equilibrium conditions become:

$$\mu_n^I = \mu_n^{II}, \tag{2}$$

$$\mu_p^I = \mu_p^{II} - \frac{\varepsilon_{surf}}{f(1-f)(\rho_p^I - \rho_p^{II})},$$
$$P^I = P^{II} - \varepsilon_{surf}\left(\frac{1}{2\alpha} + \frac{1}{2\Phi}\frac{\partial\Phi}{\partial f} - \frac{\rho_p^{II}}{f(1-f)(\rho_p^I - \rho_p^{II})}\right).$$

Note that there is an extra term in both the proton chemical potential and in the mechanical equilibrium conditions, as compared to the ones obtained in the CP approximation, Eqs. (1). These terms arise from the inclusion of the surface and Coulomb terms in the minimization of the total energy. The Coulomb repulsion induces an extra positive term while the surface tension reduces the cluster internal pressure.

3. Results

For reference and to help the discussion, we show in Table 1 the symmetric nuclear matter properties for all the models we are using in this study to compare with our calculations with the FSU interaction: another RMF parametrization, TW [28], with density-dependent couplings, and four Skyrme interactions, SkM* [29], SLy4 [30], NRAPR [31], and SQMC700 [32], chosen based on their overall performance in modelling a wide variety of nuclear matter properties [33].

Table 1. Symmetric nuclear matter properties at saturation density ρ_0 (energy per particle B/A, incompressibility K, symmetry energy E_{sym} and symmetry energy slope L) for the FSU parametrization, and five other parameter sets for comparison. All the quantities are in MeV, except for ρ_0, given in fm^{-3}.

Model	ρ_0	B/A	K	E_{sym}	L
FSU	0.148	-16.3	230	32.6	60.5
TW	0.15	-16.3	240	33	55
NRAPR	0.16	-15.85	226	33	60
SQMC700	0.17	-15.49	222	33	59
SkM*	0.16	-15.77	217	30	46
SLy4	0.16	-15.97	230	32	46

In Figure 1, we show the free energy per particle, F/A, as a function of the density. As expected, F/A is lowered when nonhomogeneous matter is present, making these states more stable. A second effect is the disappearance of the negative curvature that the EOS of homogeneous matter presents below saturation density. This effect is present in all the three methods considered. The light clusters are only present for very small densities, and will start melting for $\rho \gtrsim 0.001$ fm^{-3}. However, their presence lowers the free energy of the homogenous matter EOS and of the CP calculation, as can be seen in the inset panels. The CP approach, which does not take into account in a consistent way the surface tension and Coulomb energy, overestimates the effect of the clusterization, mainly at low densities. This problem is solved within the CLD approach, which, taking into account finite size effects in the phase equilibrium conditions, gives results closer to the TF calculation. However, there is still some overestimation of the free energy reduction with respect to the TF calculation, possibly due to the approximate description of the surface energy. Close to the crust-core transition, all approaches, TF, CP and CLD, give similar results, and predict a first-order phase transition to uniform matter.

In Figure 2, we show the chemical potential μ_B as defined in Ref. [34], $\mu_B = (1-y_p)\mu_n + y_p(\mu_p + \mu_e)$, as a function of the density on the left panel, and on the right panel, we show

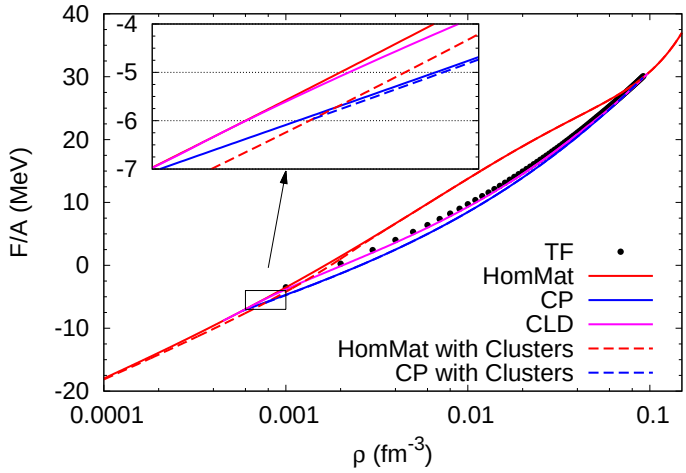

Figure 1. Free energy per baryon as a function of the density for the FSU interaction, $y_p = 0.3$, for $T = 4$ MeV. Results with pasta (within CP, CLD and TF approaches) and for homogeneous matter, and including (for homogeneous matter and pasta within CP) or not clusters, are shown. The effect of these aggregates are only seen for very small densities (inset panel).

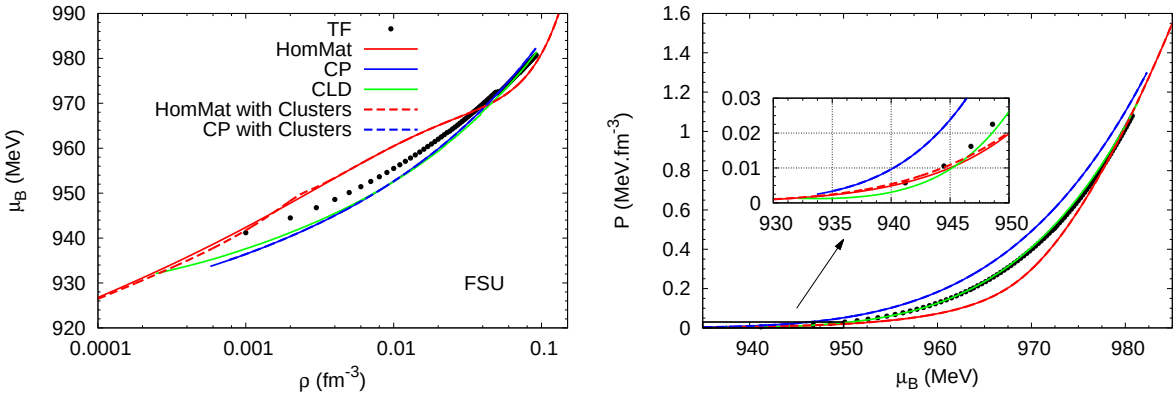

Figure 2. (Left) Chemical potential, μ_B, as a function of the density, ρ, and (right) pressure as a function of μ_b, for the FSU interaction, $y_p = 0.3$, and $T = 4$ MeV. Results with pasta (within CP, CLD and TF approaches) and for homogeneous matter, and including (for homogeneous matter and pasta within CP) or not clusters, are shown.

the total pressure as a function of μ_B. We can observe that for all the three calculations, TF, CP, and CLD, the negative curvature of μ_B is removed, just like the free energy case, shown in Fig. 1. Close to the crust-core transition, all the methods give similar results. Looking at the right panel, the pressure does not show any discontinuity when plotted against the chemical potential, μ_B, for the CLD and TF calculations. The CP method, on the other hand, presents a very large discontinuity at the onset of the pasta phase, if we look at the left panel, and at both the onset and the crust-core transition (right panel), due to the non-consistent treatment of the surface energy.

In Figure 3, we plot the entropy per particle, S/A, as a function of the density, ρ. We can see that this thermodynamical quantity is lowered with the inclusion of the pasta phases. At

very low densities, the same effect is observed when we include light clusters in the calculation for homogeneous matter.

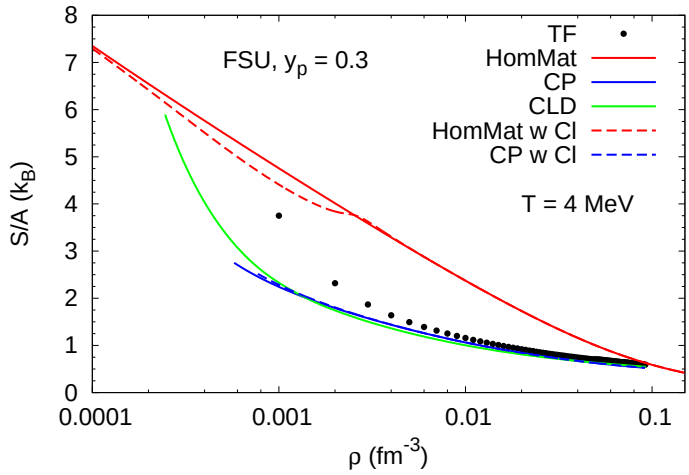

Figure 3. Entropy per particle, S/A, as a function of the density, ρ, for the FSU interaction, $y_p = 0.3$, and $T = 4$ MeV. Results with pasta (within CP, CLD and TF approaches) and for homogeneous matter, and including (for homogeneous matter and pasta within CP) or not clusters, are shown.

In Figure 4, we show the pasta phases that we obtained, within the three calculations, TF, CP, and CLD, for the FSU interaction, a fixed proton fraction of 0.3 and a temperature of 4 MeV. The slab geometries are absent in the TF calculation, except for $T = 4$ MeV, where they briefly appear. However, these heavy clusters occupy the widest density range, when performing the CP and CLD calculations. Another feature we can observe is that the density range of each shape decreases with increasing temperature. For the CLD calculation, the pasta shapes melt at $T = 10$ MeV.

It is important to stress that the appearance and density range of the different geometries is model dependent and sensitive to properties such as the symmetry energy [20]. Stable geometries depend on the parametrizations used, and the properties which influence them should be investigated.

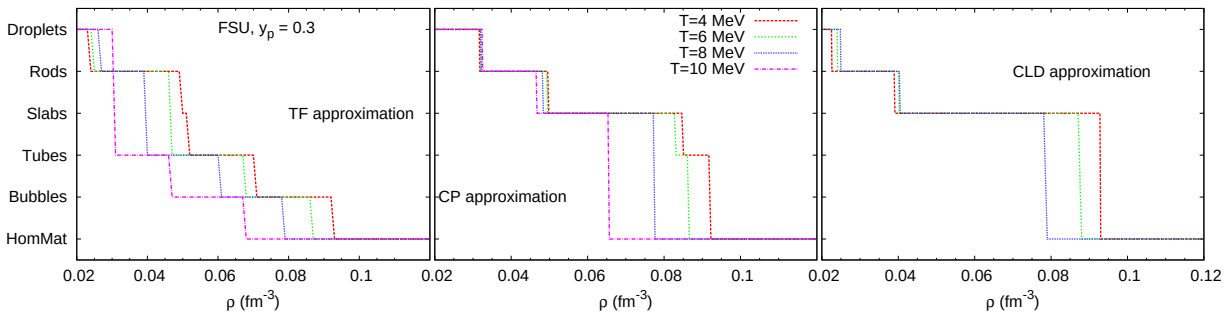

Figure 4. Pasta phases for the FSU interaction within the (left) TF, (middle) CP, and (right) CLD calculations for several temperatures. The proton fraction is fixed at 0.3.

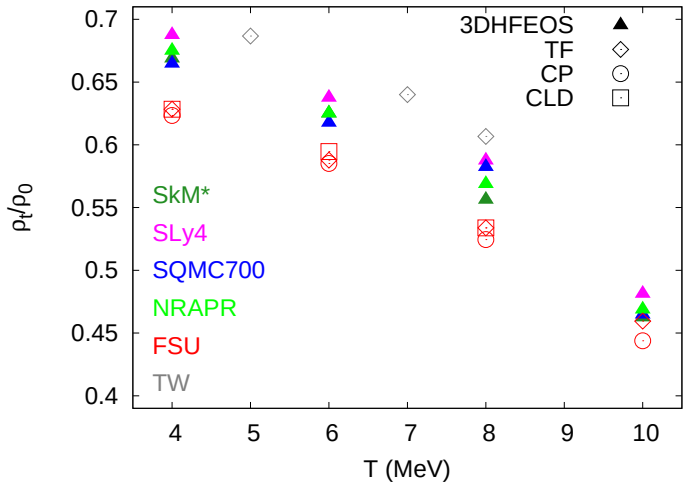

Figure 5. Crust-core transition densities, normalized to the nuclear saturation density, ρ_0, as a function of the temperature, for the 3D-HFEOS (upward triangles) calculation and the SkM* (green), SLy4 (pink), SQMC700 (blue), NRAPR (yellow) models, and the Thomas-Fermi (diamonds) calculation for the FSU (red) and TW (gray) models, and the CP (circles), and CLD (squares) results for the FSU (red) model. The proton fraction is fixed to 0.3.

In Figure 5, we show the crust-core transition densities, normalized to the nuclear saturation density, ρ_0, as a function of the temperature, for the 3D-HFEOS (upward triangles) calculation and the SkM* (green), SLy4 (pink), SQMC700 (blue), NRAPR (yellow) models, and the Thomas-Fermi (diamonds) calculation for the FSU (red) and TW (gray) models, and the CP (circles), and CLD (squares) results for the FSU (red) model. The proton fraction is fixed to 0.3. We observe that the TF, CP and CLD calculations are almost coincident. The difference to the non-relativistic calculations, 3DHFEOS, is about 0.015 fm^{-3}, and decreases with increasing temperature.

4. Conclusions

In this work, we studied the pasta geometries that appear in core-collapse supernova events and in the inner crust of neutron stars within three different approximations: the Thomas-Fermi, the coexisting phases, and the compressible liquid drop calculations, all within the single-nucleus approximation. We also introduced light clusters into our system to understand their effect on the EoS. We observed that their effect is very weak and only noticeable at very low densities. To characterize the transition to uniform matter, we plotted the free energy, pressure and chemical potential, and we reached the conclusion that the density range of the pasta phase and the crust-core transition densities decrease with increasing temperature, as expected. The stable geometries that we found depend on the parametrizations considered, and the properties that influence them should be investigated more carefully. Within the CP method, the description of the heavy clusters gives unrealistic results, as compared to the TF calculation, though it predicts concordant transition densities to uniform matter. On the other hand, the TF and CLD calculations give very similar results in the whole range of densities and temperatures considered. All the methods considered in this study show a very good agreement with respect to the transition density to homogeneous matter.

Acknowledgments
Partial support comes from "NewCompStar", COST Action MP1304. H.P. is supported by FCT under Project No. SFRH/BPD/95566/2013. She is very grateful to the Organizers of the Workshop for the opportunity to present this work and for the financial support received. S.C. is supported by FCT under project No. SFRH/BPD/64405/2009.

References

[1] Ravenhall D G, Pethick C J and Wilson J R 1983 Phys. Rev. Lett. **50** 2066
[2] Horowitz C J, Pérez-García M A and Piekarewicz J 2004 Phys. Rev. C **69** 045804
[3] Horowitz C J, Pérez-García M A, Berry D K and Piekarewicz J 2005 Phys. Rev. C **72** 035801
[4] Maruyama T, Tatsumi T, Voskresensky D, Tanigawa T and Chiba S 2005 Phys. Rev. C **72** 015802
[5] Watanabe G, Maruyama T, Sato K, Yasuoka K and Ebisuzaki T 2005 Phys. Rev. Lett. **94** 031101
[6] Sonoda H, Watanabe G, Sato K, Yasuoka K and Ebisuzaki T 2008 Phys. Rev. C **77** 035806
[7] Sonoda H, Watanabe G, Sato K, Yasuoka K and Ebisuzaki T 2010 Phys. Rev. C **81** 049902
[8] Pais H and Stone J R 2012 Phys. Rev. Lett. **109** 151101
[9] Grill F, Pais H, Providência C, Vidaña I and Avancini S S 2014 Phys. Rev. C **90** 045803
[10] Horowitz C J, Pérez-García M A, Carriere J, Berry D K and Piekarewicz J 2004 Phys. Rev. C **70** 065806
[11] Sonoda H, Watanabe G, Sato K, Takiwaki T, Yasuoka K and Ebisuzaki T 2007 Phys. Rev. C **75** 042801(R)
[12] Typel S, Röpke G, Klahn T, Blaschke D and Wolter H H 2010 Phys. Rev. C **81** 015803
[13] Horowitz C J and Schwenk A 2006 Nuclear Physics A **776** 55–79
[14] Heckel S, Schneider P P and Sedrakian A 2009 Physical Review C **80** 015805
[15] Ferreira M and Providência C 2012 Physical Review C **85** 055811
[16] Avancini S S, Barros Jr C C, Menezes D P and Providência C 2010 Phys. Rev. C **82** 025808
[17] Avancini S S, Barros Jr C C, Brito L, Chiacchiera S, Menezes D P and Providência C 2012 Phys. Rev. C **85** 035806
[18] Lattimer J M and Swesty F D 1991 Nucl. Phys. A **535** 331
[19] Shen H, Toki H, Oyamatsu K and Sumiyoshi K 1998 Nucl. Phys. A **637** 435
[20] Pais H, Chiacchiera S and Providência C 2015 Phys. Rev. C **91** 055801
[21] Todd-Rutel B G and Piekarewicz J 2005 Phys. Rev. Lett. **95** 122501
[22] Avancini S S, Chiacchiera S, Menezes D P and Providência C 2010 Phys. Rev. C **82** 055807
[23] Avancini S S, Chiacchiera S, Menezes D P and Providência C 2012 Phys. Rev. C **85** 059904(E)
[24] Avancini S S, Menezes D P, Alloy M D, Marinelli J R, Moraes M M W and Providência C 2008 Phys. Rev. C **78** 015802
[25] Baym G, Bethe H A and Pethick C J 1971 Nucl. Phys. A **175** 225
[26] Lattimer J M, Pethick C J, Ravenhall D G and Lamb D Q 1985 Nucl. Phys. A **432** 646
[27] Bao S, Hu J, Zhang Z and Shen H 2014 Phys. Rev. C **90** 045802
[28] Typel S and Wolter H H 1999 Nucl. Phys. A **656** 331
[29] Bartel J, Quentin P, Brack M, Guet C and Håkansson H B 1982 Nucl. Phys. A **386** 79
[30] Chabanat E, Bonche P, Haensel P, Meyer J and Schaeffer R 1998 Nucl. Phys. A **635** 231
[31] Steiner A W, Prakash M, Lattimer J M and Ellis P J 2005 Phys. Rep. **411** 325
[32] Guichon P A M, Matevosyan H H, Sandulescu N and Thomas A W 2006 Nucl. Phys. A **772** 1
[33] Dutra M, Lourenço O, Sá Martins J S, Delfino A, Stone J R and Stevenson P D 2012 Phys. Rev. C **85** 035201
[34] Hempel M and Schaffner-Bielich J 2010 Nucl. Phys. A **837** 210